Sensitivity analysis of a label-free detection using Opto-plasmonic nano-structured antenna

Sneha Verma
School of Mathematics, Computer Science and Engineering
City, University of London
London, United Kingdom
sneha.verma@city.ac.uk

Souvik Ghosh
School of Mathematics, Computer Science and Engineering
City, University of London
London, United Kingdom
souvik.ghosh@city.ac.uk

B.M.A Rahman
School of Mathematics, Computer Science and Engineering
City, University of London
London, United Kingdom
b.m.a.rahman@city.ac.uk

***Abstract*—This paper reports a design method of optoplasmonics sensor that consider a pair of elliptical gold nano antenna mounted on a quartz substrate. A 2D array of gold nano antenna can be used for a variety of biomedical applications due to its key electronic and optical properties which are shape and size dependent. An elliptical shaped coupled gold nano antenna with 100 nm major axis, *a* and 10 nm minor axis, *b* was optimized with separation distance, *g* and height, *h* to achieve a high sensitivity with a narrow full-width half-maximum (FWHM) and a good figure of merit (FOM). By exploiting the resonance shift of transmission spectra and high electric field confinements, the sensitivity of the proposed sensor was obtained nearly 526-530 nm/RIU and the FWHM and FOM were calculated around 110 nm and 8.1, respectively. Additionally, the proposed sensing structure have been explored to measure the 2-propanol (IPA) concentration in water.**

Keywords—nano-antenna, sensitivity, FOM, full-width half-maximum, resonating wavelength

I. INTRODUCTION

Nanotechnology has gained a significant interest in recent years because of their attractive properties such as absorption, scattering, extinction, and transmission/reflection at nanoscale. Nano structured antennas can be a good candidate for micro-level bio sensing applications due to their plasmonic properties which makes them suitable candidate for molecular sensing applications such as biomedical sensing, bio-medicines, water quality control etc. In this paper, we propose a novel coupled elliptical shaped gold nano sensor.

In 1985, Wessel published the idea of high electric field containment in tiny nano metallic particles which was observed with the help of Scanning Electron Microscopy [1]. He also discussed the presence of surface plasmon resonance of nanoparticles. The effect of various shapes and device parameters of the plasmonic antenna for a variety of applications was reported. In 2004, Atay *et al.*, [2] described periodic array of circular gold nanoparticles with powerful resonance and far-field patterns. Surface Enhanced Raman Spectroscopy (SERS) is also an important technique to visualize the performance of the nano antennas and D'Andrea *et al.* [3] reported a nanostructure which can resonate in both ultraviolet and visible regions at the same time. The importance of computational modeling and experimental investigations towards strong resonance and versatile field confinement have indeed been reported in recent years. Some numerical techniques, such as finite element method [FEM] [4]–[7] and finite difference time domain method [FDTD] [8], [9], have been used to model the architecture of gold nano antennas.

The paper is divided as follows: Section II discusses the background theory of the designed sensor. Section III discusses the Numerical Methods and design optimization, with four subsections detailing the efficiency of the designed nanostructure and its application for detecting the aqueous solutions of 2-propanol (IPA). Finally, in Section IV a conclusion is drawn.

II. NUMERICAL METHODS AND MODEL OPTIMIZATION

A. Principle of Gold Nano Metallic Structures for Sensing Applications

In this work, the frequency domain plasmonic field distribution of the coupled gold nanoparticles is characterized by using the FEM. Drude Lorentz model was used to calculate the dielectric property of gold because it emphasizes on the presence of free-electrons in metals, which induces surface plasmons resonance. Dielectric constant of gold was calculated by using the Drude free-electron theory and shown below [10]:

$$\varepsilon_{real} + \varepsilon_{imag} = 1 - \frac{{\omega_p}^2\tau^2}{1+\omega^2\tau^2} + \frac{{\omega_p}^2\tau}{\omega(1+\omega^2\tau^2)} \quad (1)$$

For metals at near-infrared frequencies when $\omega \gg 1/\tau$, Eq. (1) simplify to [10].

$$\varepsilon(\omega) = 1 - \frac{{\omega_p}^2}{\omega^2} + j\frac{{\omega_p}^2}{\omega^3\tau} = \varepsilon_{real}^f + \varepsilon_{imag}^f \quad (2)$$

Here, ω_p is the plasma angular frequency equal to $\sqrt{\frac{4\pi Ne^2}{m_0}}$, where N and m_0 are the conduction electron density and effective optical mass, respectively, and τ is the relaxation time. This can be separated into its real and imaginary parts of the dielectric constant [10]. To investigate the plasmonic properties, the conventional Maxwell equation is solved by using the FEM after considering the time harmonic dependence of Electric field $E(r,t) = E(r)e^{-j\omega t}$. Helmholtz equation can be derived from the Maxwell's equations and shown below,

$$\nabla^2 E + {k_0}^2 \varepsilon E = 0 \quad (3)$$

Where $k_0 0$ is the wavevector and the time harmonic the propagating field is defined as E (x, y, z) = E (x, y, z) ej$^{\beta z}$ and where β is the propagation constant. In complex form γ = α+jβ, if α = 0 then γ = jβ represents the propagation dependence in the z direction.

III. Numerical Observations of Structural Configuration of the Coupled Nano Antenna

A. Parameters used for Numerical Simulation/Calculations

The FEM approach is used here to obtain the numerically simulated results by using a commercial software, COMSOL Multiphysics 5.5. In this work, the unit cell of the coupled elliptical shaped nano antenna have been considered in order to reduce the computation time. To design the paired antenna structure, Perfect Magnetic Conductor (PMC) and Perfect Electric Conductor (PEC) have been enforced along the x and y directions, respectively. Perfectly matched layers (PML) with a height of 200 nm were also added at the top of the air domain and at the base of the quartz substrate to prevent back reflection artifacts in the simulations. The antenna have been illuminated from the top with a x-polarized electric field propagating in the z directions. The entire numerical simulation has been solved by using RF model frequency domain scattered field distributions.

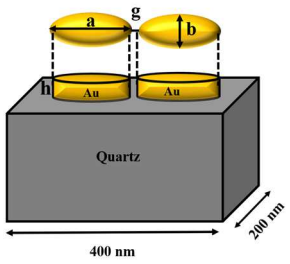

Fig. 1. Schematic of paired nano-antenna unit cell.

The schematic array of the paired gold nano-structured antenna on a quartz substrate is shown in Fig. 1. The dimensions of the unit cell was taken as 400x200 nm^2. This figure also shows the major axis, a, minor axis, b and separation gap g of the nano structures. Through optimizing the computational model, the antenna dimensions have been determined, in order to achieve a high sensitivity value

B. Numerical Outcomes

Localized Surface Plasmon Resonance (LSPR) plays an important role in the excitation state of any plasmonics antenna because of their response dependence on the environmental medium. The transmission spectra have been calculated for different surrounding refractive indices to observe the shift in the resonating wavelength. It is observed that the resonating wavelength shifts prominently with the surrounding refractive indices, hence it can be used as a RI sensor as shown in Fig. 2(a).

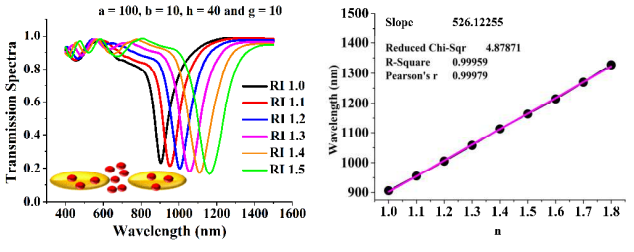

(a) (b)

Fig. 2. (a) Transmission spectra of the optimized paired elliptical antenna for various surrounding RIs. (b) Sensitivity and R-Square Error calculation for the optimized structure.

To calculate the sensitivity (nm/RIU), S of the designed structure which is defined as the ratio of resonant wavelength λ_{res} shift with the change in environmental refractive index δn_s (RIU):

$$S = \frac{\lambda_{res}(\text{nm})}{\delta n_s(\text{RIU})} \tag{4}$$

Its sensitivity has been calculated by using Eq. (3) and R-square error was calculated as 0.9959, which shows an almost linear wavelength shift at different RI. Variation of the resonating wavelength shift with the surrounding RI is shown in Fig. 2(b). From this, it can be observed that nearly 526-530 nm/RIU sensitivity can be achieved for the optimized structure. Hence, it can be considered as a good candidate for molecular sensing applications.

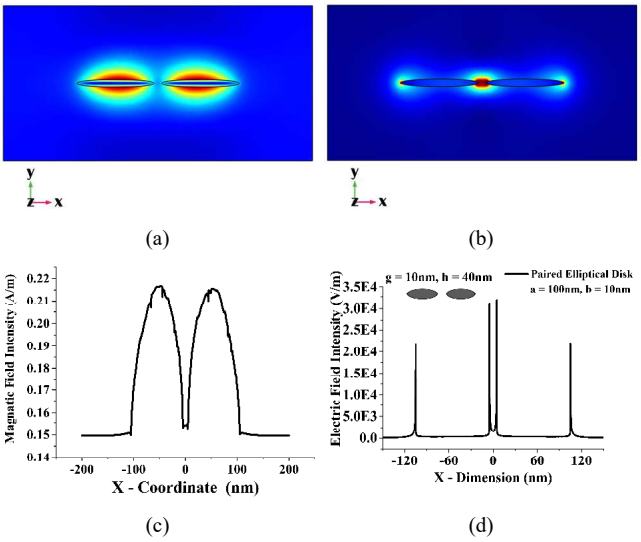

(c) (d)

Fig. 3. (a) Modal *Hx*. (b) *Ex* fields. (c) Magnetic field intensity of the optimized structure along the x-axis. (d) Electric field intensity of the elliptical nano shaped antenna.

To understand the performance of such nano antennas, both the dominant magnetic and electric fields are shown in Fig. 3. The dominant H_x contour is shown in Fig. 3(a), and it can be observed that H_x field is confined in both the metallic antenna. On the other hand, E_x contour shown in Fig. 3(b), where it can be clearly observed that E_x field is higher along the 4 narrow corners of this elliptical dimer. The E_x field profile for a single circular antenna (not shown in paper) is also circularly symmetric. But, for an elliptical antenna, due to lack of this circular symmetry, the field is more localized and makes elliptical shaped antenna more sensitive. Two slightly enhanced peaks can be seen at the outer edges and a much-enhanced field in the gap region. To see this more clearly, the variation of H_x and E_x along the x-axis through the center of the antenna is shown in Figs. 3(c) and 3(d), respectively. It can be noted that H_x field is maximum at the centre of the metallic antenna and almost zero in the gap. On the other hand, E_x variation shown in Fig. 3(d) clearly shows 4 peaks at the edges of the narrow ends. However, the field intensity in the gap area is much higher than the outer edges and thus makes such dimer much more efficient. From this it is clear that the electric field confinement of the paired elliptical disk is increased significantly as compared to the paired circular disk which has a great potential for sensing applications.

C. *Full Width at Half Maximum (FWHM) and Figure of Merit Optimization*

To design an efficient sensor, measurement accuracy also plays an important role, which depends on the sharpness of the resonance curve and this can be quantified by the FWHM, which is defined as the difference between two wavelengths, where response is half of its maximum value as shown by Eq. (5).

$$FWHM = \lambda_1 - \lambda_2 \tag{5}$$

where λ_1 and λ_2 are the wavelengths, when the transmission is half of its maximum value. From this the FWHM has been calculated as 110 nm. Subsequently, we can evaluate different designs depending on its FWHM values. As in such sensors, we prefer to have a high sensitivity, *S*, and also a sharper resonance (that is smaller FWHM) so the Figure-of-Merit (FOM) can be considered as an important parameter for the design of a Paired nano antenna array. This, FOM can be defined as ratio of the sensitivity to the FWHM:

$$FOM = \frac{S(nm/RIU^{-1})}{FWHM} \tag{6}$$

Finally, FOM of the optimized deign has been calculated as 8.1 from the Eq. 6.

D. *Model Investigation and Its Applications*

In this paper, optimized design has been used to show the efficient performances in terms of sensitivity and FWHM and next, this design has been tested for detection of 2-propanol (IPA) concentration through its corresponding refractive indices, which are adopted form [11], and shown in Table I.

TABLE I. REFRECTIVE INDICES OF AQUEOUS SOLUTION OF 2-PROPANOL (IPA)

C	0%	10%	20%	40%	60%	80%	100%
RI	1.3330	1.3420	1.3514	1.3642	1.3713	1.3742	1.3776

Fig. 4(a) shows the transmission spectra of aqueous solution of 2-propanol (IPA) at different concentrations where the black, pick, blue and orange curves show the 0%, 20%, 60%, and 100% IPA concentration, respectively. Fig. 4(b) shows the calculated FWHM with the IPA concentration having different refractive indices. From this figure it can be observed that at different IPA concentration (shown by pink dots) the FWHM was calculated as ~135 nm; however, it increases for higher refractive index values as shown by a black curve. On the other hand, Fig. 4(c) shows the resonating wavelength with the refractive indices by a black curve with its highest value nearly 1320 nm at 1.8. In this figure, the variations of resonating wavelength for IPA solution are also shown by pink dots at around 1100 nm. Fig. 4(d) shows the plasmonic wavelength shift of antenna placed in IPA solution compared to its placement in the vacuum. To calculate the value of the shifted plasmonic wavelength, the plasmonic resonating wavelength (when antenna was presented in inert environment) was subtracted from the wavelength (when antenna was presented in different concentration of IPA as shown in Fig. 4(d). In this way, the potential application in detection of IPA aqueous solution at different concentrations from 0% to 100% has been shown by a black curve in Fig. 4(d). Pink dashed lines show the corresponding refractive index of aqueous solution of IPA at different concentrations from 0% to 100% with respect to resonating wavelength. A strong argument can be made here that the optimized design can be a useful candidate for many homogeneous RI sensing applications.

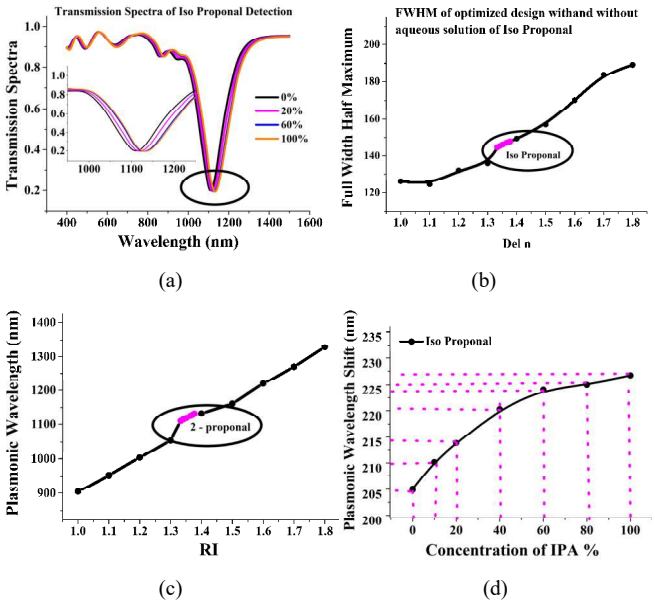

Fig. 4. (a) Shows the transmission spectra of different IPA concentrations. (b) Demonstrate the FWHM variation of 2-propanol (IPA) with different RIs. (c) Shows the resonating plasmonic wavelength with refractive index values. (d) Shows the shift in resonating wavelength with the 2-propanol (IPA) concentration.

Hence, this presented RI sensing scheme shows the trade-off between defined LSPR measurement and high sensitivity caused by coupled periodic antenna and shows its promising results for liquid refractive index sensing such as observing water quality and its characterization and biomedical application where liquid sensing is in high demand.

IV. CONCLUSION

Numerical simulated results show that the shape of nanoparticles has a significant impact on the properties of nano-optical antennas. We have also optimized the design which in this case considered an array of gold nano-structures with a = 100 nm, b = 10 nm, g = 10 nm and h = 40 nm. The sensitivity of the optimized plasmonic sensor has been determined by the shift of the transmission spectra. The sensitivity, FWHM and FOM were calculated as 526 nm/RIU, 110 nm and 8.1, respectively. Furthermore, the adopted design shows a high electric field distribution in the gap region. After successfully optimizing the nano antenna as a sensor, an aqueous solution at various IPA concentrations was used to observe the sensitivity of the engineered sensor, demonstrating its significant contribution to the advancement of potential innovative technologies for Point-of-Care, therapeutic, and water quality assessments, as well as a tool for regulating seawater salinity.

ACKNOWLEDGMENT

Authors would like to thank to City, University of London. This work was supported in part by the City, University of London Doctoral Fellowship program and S.V also would like to thank to Worshipful Company of Scientific Instrument Makers for providing some part of the funding.

REFERENCES

[1] J. Wessel, "Surface-enhanced optical microscopy," J. Opt. Soc. Am. B, vol. 2, pp. 1538-1541, 1985.

[2] T. Atay, J. H. Song, and A. V. Nurmikko. "Strongly interacting plasmon nanoparticle pairs: from dipole-dipole interaction to conductively coupled regime," Nano Letters, vol. 4, no. 9, 2004, pp. 1627-1631.

[3] C. D'Andrea, J. Bochterle, A. Toma, C. Huck, F. Neubrech, E. Messina, B. Fazio, O. M. Marago, E. Di Fabrizio, M. L. Chapelle, P. G. Gucciardi and A. Pucci, "Optical nanoantennas for multiband surface-enhanced infrared and Raman spectroscopy," ACS Nano, 7(4), 2013, pp.3522-3531.

[4] R. M. Bakker, V. P. Drachev, Z. Liu, H. K. Yuan, R. H. Pedersen, A. Boltasseva, J. Chen, J. Irudayaraj, A. V. Kildishev and V. M. Shalaev, "Nanoantenna array-induced fluorescence enhancement and reduced lifetimes," New Journal of Physics 10(12), 2008, 125022.

[5] Z. Liua, A. Boltasseva, R. H. Pedersen, R. Bakker, A. V. Kildisheva, V. P. Drachev and V. M. Shalaeva, "Plasmonic nanoantenna arrays for the visible," Metamaterials, 2(1), 2008, pp. 45–51.

[6] J. Caldero´n, J. A´ lvarez, J. Martinez-Pastor and D. Hill, "Polarimetric plasmonic sensing with bowtie nanoantenna arrays," Plasmonics, 10(3), 2015, pp. 703–711.

[7] J. Caldero´n, J. A´ lvarez, J. Martinez-Pastor and D.Hill, "Bowtie plasmonic nanoantenna arrays for polarimetric optical biosensing," InFrontiers in Biological Detection: From Nanosensors to Systems VI, Vol. 8933, 2014, p. 89330I, [International Society for Optics and Photonics].

[8] O.Limaj, D. Etezadi, N.J. Wittenberg, D.Rodrigo, D. Yoo, S. H. Oh and H. Altug, "Infrared plasmonic biosensor for real-time and labelfree monitoring of lipid membranes," Nano Letters, 16(2), 2016, pp. 1502–8.

[9] B.Mehta and M. E. Zaghloul, "Effect of rounding on the sensitivity of optical antennas based sensors," In SENSORS, 2014 IEEE, pp. 1391-1394.

[10] P. B. Johnson and R. W. Christy, "Optical constants of the noble metals," Physical Review B, 6(12), 1972, 4370.

[11] N. Laman and D. Grischkowsky, "Terahertz conductivity of thin metal films," Applied Physics Letters, 93(5), 2008, 051105.